Experimental study of the transitional flow regime in coiled tubes by the estimation of local convective heat transfer coefficient

Experimental study of the transitional flow regime in coiled tubes by the estimation of local convective heat transfer coefficient

Luca Cattani[a], Fabio Bozzoli[a,b], Sara Rainieri[a,b]
[a] SITEIA.PARMA Interdepartmental Centre, University of Parma,
Parco Area delle Scienze 181/A, I-43124 Parma, Italy
[b] Department of Industrial Engineering, University of Parma,
Parco Area delle Scienze 181/A I-43124 Parma, Italy

E-mail of the corresponding Author (Luca Cattani): luca.cattani@nemo.unipr.it

Abstract. The present work is focused on studying the transition between the laminar and turbulent flow regime in coiled tubes. Wall curvature is a popular heat transfer enhancement technique since it gives origin to the centrifugal force in the fluid. This phenomenon, both in the laminar and the turbulent flow regime, promotes local maxima in the velocity distribution that locally increase the temperature gradient at the wall by enhancing the heat transfer and, at the same time, leading to a significant variation in the convective heat-transfer coefficient along the circumferential angular coordinate. However, this geometry delays the transition from laminar to turbulent regime, transition that, in the majority of the papers available in the scientific literature, has been investigated on the basis of pressure drop data behaviour. In the present work the estimation of the local convective heat transfer coefficient distribution, based on the solution of the inverse heat conduction problem in the tube's wall, is proposed as a complementary and detailed tool to investigate the transitional flow regime. Moreover, the present research gives additional information on the phenomenon of the transition in coiled tubes by monitoring the local convective heat transfer coefficient.

Keywords: transition to turbulence, coiled tubes, local convective heat transfer coefficient, inverse heat conduction problem.

1. Introduction

Wall curvature is one of the most frequently used techniques to enhance the convective heat transfer [1,2] since it gives origin to the centrifugal force in the fluid: this phenomenon induces local maxima in the velocity distribution that locally increase the temperature gradient at the wall by maximising the heat transfer [3-5]. Dean [6-7] solved the simplified Navier–Stokes equations for a coiled pipe of small curvature showing that the flow is governed by the Dean number $De = Re \cdot \delta^{0.5}$, where Re is the Reynolds number and δ is the curvature ratio, defined as the ratio of the pipe diameter to the coiling diameter. Moreover, the curvature induces a secondary flow that causes the fluid to be pushed from the tube core region toward the outer wall where it bifurcates and drives the fluid near the wall toward the inner wall of the tube, thus forming a pair of recirculating counter-rotating vortices, usually named as Dean vortices. This promotes an additional convective transport that increases both the heat transfer and the pressure drop with respect to the straight tube behaviour.

Both in the laminar and the turbulent flow regime, the curvature produces an irregular distribution of the velocity field over the cross-section of the tube which leads to a significant variation in the convective heat-transfer coefficient along the circumferential angular coordinate: it presents higher values at the outer bend side of the wall surface than at the inner bend side [5,8,9].

For what concern the transitional regime in coiled tubes, to the present Authors' knowledge, there are neither experimental nor numerical data in terms of local heat transfer coefficient, although, in curved pipes, the process of transition to turbulence differs qualitatively from that in straight ones.

Almost the totality of the tests performed with the purpose of detecting the transition to turbulence in coiled tubes concerned the analysis of pressure drop characteristics. In the early studies on this topic, the earlier departure from the linear pressure drop/flow rate behaviour observed in curved tubes with respect to straight pipes, was interpreted as an indication of the transition to turbulence [10]. Dean [6,7] with his work otherwise demonstrated that this departure from the linearity in the relationship between the pressure drop and the flow rate wasn't the signal of an anticipated transition to turbulence but an indication that the flow in curved tubes is not self-similar [10]. On the other hand, it is currently accepted that coil curvature suppresses turbulent fluctuations arising in the flowing fluid, smoothing the emergence of turbulence and increasing the value of the Reynolds number required to attain a fully turbulent flow, with respect to a straight pipe [10,11].

White [12] in his experimental work, analysed pipes with different curvature ratio δ and described the existence of a critical Reynolds number that defines the emergence of turbulence. Many other studies [13-16] were carried out on the same topic and they all pointed out that the flow in curved pipes remains laminar up to Reynolds numbers higher at least by a factor of two than in straight pipes.

Ito [15] conducted a wide set of experimental tests for an ample range of curvature ratio and Reynolds number values investigating the transition to turbulence. The experimental results were reduced in order to find the following equation for the critical Reynolds number value:

$$Re_{cr} = 2000 \cdot \left(1 + 13.2 \cdot \delta^{0.6}\right), \qquad (1)$$

valid in the range $5 \cdot 10^{-4} < \delta < 0.2$.

Also the paper of Srinivasan et al. [16] showed that the effect of curvature is to delay transition to turbulence with respect to straight pipes finding a similar correlation for the critical Reynolds number in curved tubes.
Cioncolini and Santini [11] carried out an experimental analysis of the friction factor in helical pipes in an wide range of curvature ratio and of Reynolds number. For values of curvature ratio higher than 0.0416 the transition to turbulence was more gradual than in straight pipes and it was indicated only by a change in slope of the curve of the friction factor as a function of Reynolds number. The critical Reynolds number value was approximated by the following equation:

$$Re_{cr} = 3 \cdot 10^4 \cdot \delta^{0.47}, \tag{2}$$

in the range $0.0416 < \delta < 0.143$.
Moreover, they found that the transition exhibits a more complex behaviour for lower curvature ratio values ($2.7 \cdot 10^{-3} < \delta < 0.0416$). The friction factor presents a first discontinuity in correspondence of:

$$Re_{cr,I} = 12500 \cdot \delta^{0.31}. \tag{3}$$

Beyond this point, the friction factor profile exhibits a local minimum followed by a local maximum; this second discontinuity was individuated by the following equation:

$$Re_{cr,II} = 120000 \cdot \delta^{0.57}. \tag{4}$$

After this second discontinuity the slope of the friction factor presented a constant profile marking in this way the end of the turbulence emergence process [11].
For what concern the thermal analysis, to the present authors knowledge, there are not any works that investigate the transition between laminar and turbulent flow regimes throughout the study of neither the average nor the local heat transfer coefficient.
Nevertheless, many authors investigated either the laminar or the turbulent regimes in terms of average Nusselt number finding various correlations that, even if they don’t focus on the specific study of the transition, remark a distinction between the two regimes. A wide review on helically coiled tubes and other curved pipes was conducted by Naphon and Wongwises [3].
Rainieri et al. [17] studied experimentally the forced convective heat transfer in helically coiled tubes with different curvature ratio values in the Reynolds and Dean number ranges 70-1200 and 12-290 respectively, by adopting ethylene glycol as working fluid. The experimental data were correlated by considering a dependence of the Nusselt number on the curvature ratio, Reynolds and Prandtl numbers for the helically coiled tubes. Also Xin and Ebadian [18] investigated experimentally the heat transfer and the fluid motion inside helically coiled pipes both in the laminar and turbulent regimes. The study was carried out adopting different fluids (air, water and ethylene glycol) on five uniformly heated helical pipes with different geometrical parameters (pipe diameter and pitch to coil diameter ratio).
The behaviour of the helically coiled tubes in turbulent regime was analysed also by Yildiz et al. [19] and the effect of placing spring-shaped wires inside that tubes was considered.
Both the average Nusselt number and the local Nusselt number have been never adopted in literature as an instrument to analyse the transition between laminar and turbulent flow regimes.

In the present work the local convective heat transfer coefficient distribution analysis is proposed as a complementary and detailed tool to investigate the transitional regime.
The estimation procedure presented in [20], is hereby applied to estimate the local convective heat-transfer coefficient at the fluid-wall interface in coiled tubes: the temperature distributions on the external wall of the coiled tube, acquired using the infrared technique, are adopted as input data of the inverse heat conduction problem in the wall of the pipe.
The local convective heat transfer coefficient has been already investigated in the past but nevertheless, to the Authors' knowledge, only five papers [18,20-23] have presented experimental results and only three of them reported the actual local values for the convective heat transfer coefficient [20-22] while the others, neglecting heat conduction in the tube wall, estimated only apparent values [18, 23].
Bai et al. [21] experimentally found that the local heat-transfer coefficient was not evenly distributed along the periphery of the cross section and that, in particular, at the outside surface of the coil, it was three or four times higher than that at the inside surface.
Bozzoli et al. [20] focused their investigation on the fully developed region for the laminar flow regime showing that, at the outside surface of the coil, the Nusselt number was approximately five times larger than that at the inside surface and this ratio, in the conditions under test, was independent of *Re*.
Regarding local heat-transfer coefficient, some experimental data were discussed by Seban et al. [22] investigating the laminar flow of oil and the turbulent flow of water in coils. These Authors correctly drew the attention to the difference between apparent and true local values: apparent heat transfer coefficient were obtained neglecting the circumferential heat conduction in the tube wall, that means considering the average value of the convective heat flux instead of the local value. In terms of true heat transfer coefficient, the ratio of the outside to the inside coefficient found in this experimental campaign was about four for both the laminar flow case and the turbulent flow case. However, no details about the approach adopted to estimate the local convective heat flux were given in this paper.
Extending the bibliographical research to the numerical approaches, there are many others papers in which heat-transfer coefficient distributions are estimated for a wide range of conditions.
In particular, the laminar fluid flow in coiled tubes was locally investigated in [24-30]. Among these papers, the results of Yang et al. [29] are particularly relevant: the Authors presented a numerical investigation on the fully developed laminar convective heat transfer in a helicoidal pipe, with particular attention to the effects of torsion on the local heat-transfer coefficient. In particular, these Authors reported the Nusselt number distribution varying the coil pitch, and they showed that, due to torsion, the local heat-transfer coefficient, compared to the case of an ideal torus, is increased on half of the tube wall while it is decreased on the other half.
Regarding the turbulent fluid flow in coiled tubes numerical results, reported in terms of local heat-transfer coefficient, are present in [31-35]. The papers of Jayakumar et al. [32], Di Piazza and Ciofalo [33] are particularly interesting. Jayakumar et al. [32] numerically analysed the turbulent heat transfer in helically coiled tubes and presented the local Nusselt number at various cross sections along the curvilinear coordinate. The results showed that, on any cross section, the highest Nusselt number is on the outer side of the coil, and the lowest one is expected on the inner side. Moreover, these Authors proposed a correlation for predicting the local Nusselt number as a function of the average Nusselt number and the angular location for both the constant temperature and the constant heat-flux boundary conditions. Di Piazza and Ciofalo [33] obtained computational results for turbulent flow and heat transfer in curved pipes,

representative of the configuration found in helically coiled heat exchangers. Following a grid refinement study, grid independent predictions from alternative turbulence models (k–ε, SST k–ω and RSM–ω) were compared with direct numerical simulation results and experimental data also in terms of local convective heat-transfer coefficient.
In the present work the estimation of the local convective heat transfer coefficient distribution based on the inverse problem data processing approach applied to infrared thermographic maps, is proposed as a powerful tool to investigate the transitional flow regime.

2. Experimental setup and Estimation Procedure

A helically coiled stainless steel type AISI 304 tube was tested: it presented smooth wall and it was characterised by eight coils following a helical profile along the axis of the tube. The tube internal diameter was 14 mm, and the wall thickness measured 1.0 mm. The helix diameter was of approximately 310 mm while the pitch was about 200 mm. This geometry yields a coiled pipe length L of approximately 8 m and a dimensionless curvature δ of 0.045.
The working fluid was conveyed by a volumetric pump to a holding tank, and it entered the coiled test section equipped with stainless-steel fin electrodes, which were connected to a power supply, type HP 6671A. This setup allowed investigating the heat transfer performance of the tube under the prescribed condition of uniform heat flux generated by the Joule effect in the wall.

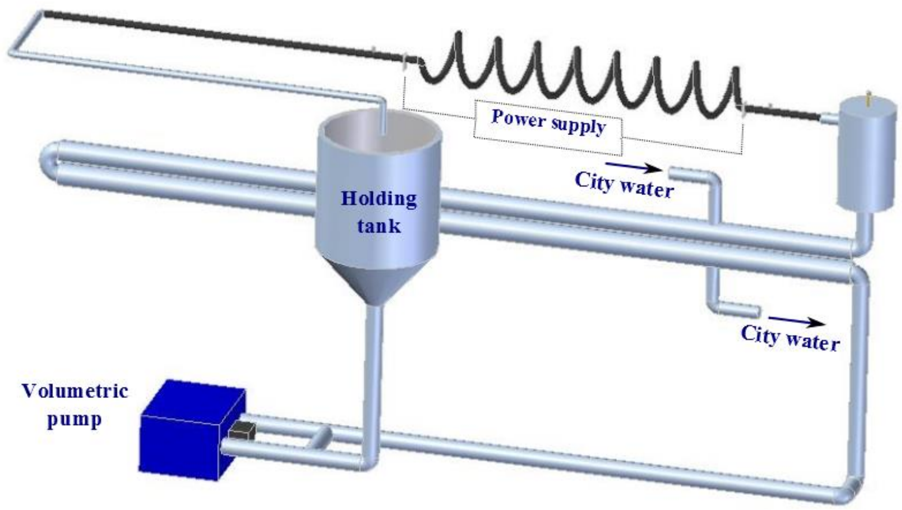

Figure 1. Sketch of the experimental setup.

Further details on the experimental setup, sketched in Fig.1, are given in [5].
To investigate the heat transfer performance of coiled tubes in the laminar, transitional and turbulent flow regime, water was used as working fluid in the Reynolds number range 300−15000. In the temperature range characterising the experimental conditions, the Prandtl number of the working fluid varied in the range of 5-9.
The investigation was firstly devoted to measure the average performance of the coiled pipes in terms of both the heat transfer effects and the pressure drop penalties.
The whole length of the heat transfer section was thermally insulated to minimize the heat transfer to the environment. Both the wall and the inlet fluid temperature were measured through type T thermocouples. Regarding the wall temperature, the sensors were attached at

different circumferential locations to the external tube's surface and at different axial locations along the heated section. In particular, the thermocouples were placed along the external and internal side of the coil. The inlet temperature was measured by a thermocouple probe placed on the tube's wall upstream the starting heating section. The bulk temperature at any location in the heat transfer section was calculated from the energy balance on the heated pipe as follows, by assuming the power supplied in the tube wall distributed uniformly per unit length over the heat transfer surface area:

$$T_b = \frac{Q}{\dot{m} \cdot c_p} \cdot \frac{z}{L} + T_e \tag{5}$$

where Q is the heat power provided to the pipe, $\dot{m}$ and c_p are the fluid mass flowrate and specific heat, respectively, T_e is the bulk temperature of the fluid at the inlet section of the coil, L is the coiled pipe length and z is the distance from the inlet section of the coil, taken along the curvilinear coordinate.

Pressure drop throughout the coiled section was measured in isothermal conditions by a Rosemount-3051S differential pressure transducer.

For the tests performed to estimate the local heat transfer a small portion of the external tube wall was made accessible to a thermal imaging camera by removing the thermally insulating layer, and the wall portion was coated with a thin film of high emissivity paint. Starting from the temperature distribution acquired on the external wall surface it was possible to estimate the local convective heat transfer coefficient at the fluid-internal wall interface by solving the Inverse Heat Conduction Problem (IHCP) in the wall.

As it is well known, however, this procedure approach presents some complications due to the fact that the IHCP is an ill-posed problem and, consequently, it is very sensitive to small perturbations in the input data. In order to bypass the ill-posedness of inverse problems, many techniques based on the processing of the experimental data have been suggested and validated in literature.

Among these techniques, the function specification methods [36,37], iterative methods [38–40], methods based on filtering proprieties [41–44], regularisation techniques [45-49] and probabilistic methods [50,51] are found. Regarding the regularisation techniques, Tikhonov regularisation method [46] is one of the most commonly employed.

In order to estimate the local convective heat transfer coefficient, the procedure presented in [20] was adopted. The temperature distribution maps on the external coil wall were employed as input data of the linear inverse heat conduction problem in the wall under a solution approach based on the Tikhonov regularisation method. The surface temperature distribution was acquired by means of a FLIR SC7000 unit, with a 640 x 512 pixel detector array. Its thermal sensitivity, as reported by the instrument manufacturer, is 20 mK at 303 K, while its accuracy is ±1 K.

To measure the temperature distribution on the whole heat-transfer test section surface, multiples images were acquired, moving the infrared camera around the section, and they were conveniently cropped, processed by perspective algorithms and merged together in Matlab® environment to obtain continuous temperature functions on the tube wall versus the circumferential angular coordinate. A sketch of the laboratory facility is shown in Fig. 2.

a)

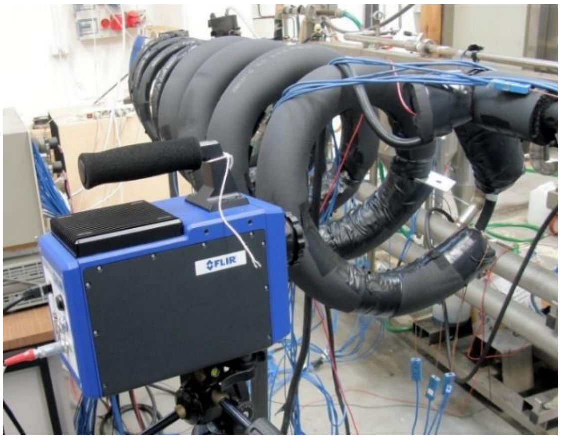

b)

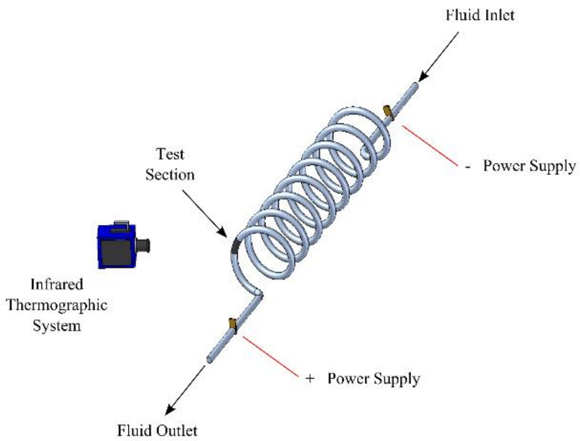

Figure 2. Picture (a) and sketch (b) of the laboratory facilities.

The estimation procedure is based on a simplified 2-D model of the test section (sketched in Fig. 3) formulated by assuming that the temperature gradient in the tube wall is almost negligible along the axis of the tube.

a)

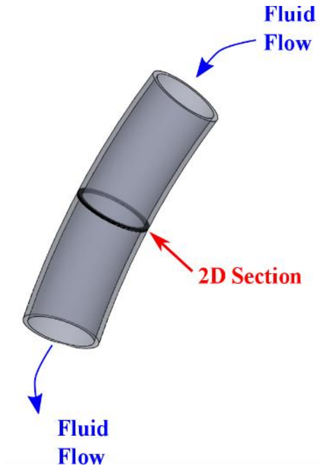

b)

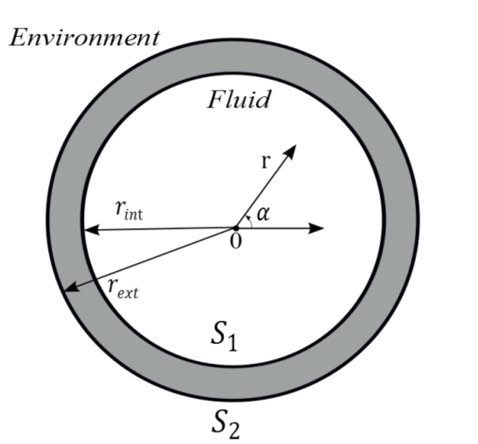

Figure 3. Coiled section (a) and 2-D model of the test section (b).

The direct formulation of the problem is concerned with the determination of the temperature distribution on the tube external wall when the convective heat flux on the tube internal wall is known. In the inverse formulation considered here, the convective heat flux is instead regarded as being unknown, whereas the surface temperature is measured.

As the inverse problem is ill-posed, in order to cope with the presence of noise in the measured temperature, some type of regularisation is required. The Tikhonov regularisation method, successfully applied in the inverse heat-transfer literature [46, 47, 52, 53], makes it possible to reformulate the original problem as a well-posed problem by minimising a specified objective function that represents a trade-off between the fidelity of the fit and the stability of the solution. The best balance between these two goals it is obtained in this paper by the adoption of the fixed-point method proposed by Bazán and co-workers [52, 53].

Once the heat-flux distribution at the fluid-wall interface compatible with the experimental temperature data has been determined through this strategy, described in detail in [21], the local convective heat transfer coefficient can be easily determined, as follows:

$$h(\alpha) = \frac{q(\alpha)}{T(\alpha, r = r_{\mathrm{int}}) - T_b}, \tag{6}$$

where $q(\alpha)$ is the heat flux distribution estimated under the solution approach based on the Tikhonov regularisation method with the support of fixed-point iteration techniques, $T(\alpha, r=r_{int})$ is temperature distribution on the tube internal wall, efficiently estimated by numerically solving the direct problem by imposing a convective heat flux equal to $q(\alpha)$ and T_b is the bulk-fluid temperature at the test section.

3. Results and discussion

The experimental conditions were designed in order to estimate the local convective heat transfer coefficient (Eq. (6)) in coiled pipes not only in transitional flow regime but also in laminar and turbulent flow regimes. The tests were performed by varying the Reynolds number. According to the correlations reported in Eqs. (1,2), the values of the critical Reynolds number, for the geometry considered in this work, varies in the range $6000 < Re_{cr} < 7500$.
Before analysing the local convective heat transfer characteristics of the coiled tubes, it was investigated how the curvature impact on the overall thermo-fluid dynamics performance of the pipes under test at different flow regimes.

3.1 Average Thermal and fluid dynamics performance

The heat transfer performance and the pressure drop penalty were quantified by means of the Nusselt number and Darcy friction factor respectively defined as follows:

$$Nu = \frac{h \cdot D}{k_f} \tag{7}$$

$$f = \frac{\Delta p}{\rho} \cdot \frac{D}{L} \cdot \frac{2}{w^2} \tag{8}$$

where k_f is the fluid thermal conductivity, w is the mean fluid axial velocity and Δp is the pressure drop along the coiled section having length L. The asymptotic Nusselt number, which is reached in the downstream region of the heated section, is reported in Fig. 4 vs. the Reynolds number. In the same figure the correlations proposed by Rainieri et al. [17] for laminar regime and by Yildiz et al. [19] for turbulent regime in helical coiled pipes are shown. In order to take into account the adoption of different fluids to obtain the various correlations, the Nusselt number values were divided by $Pr^{0.4}$.

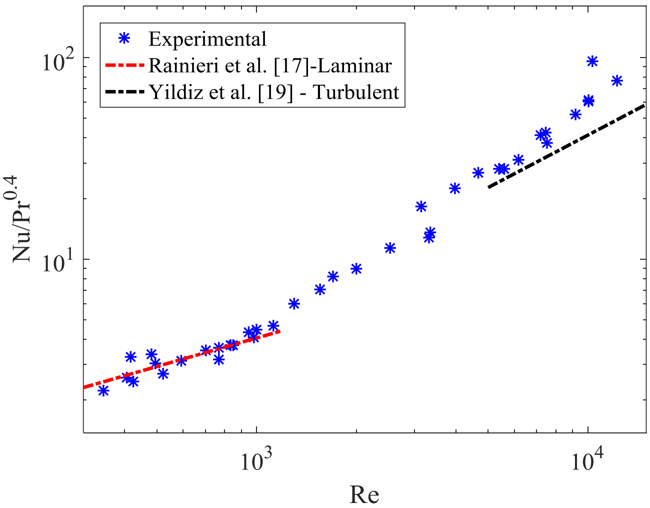

Figure 4. Asymptotic Nusselt number vs. Reynolds number for the helically coiled tube under test and comparison with the correlations proposed by Rainieri et al. [17] for laminar regime and by Yildiz et al. [19] for turbulent regime.

The data reported in Fig. 4 show a satisfying correspondence with both the correlations proposed by Rainieri et al. [17] for laminar regime and by Yildiz et al. [19] for turbulent regime, respectively. The transitional regime results more difficult to be identified by the average Nusselt number because only a slight change of slope is possible to be appreciated in the range $1000 < Re < 2000$.

In Fig. 5 the average Darcy friction factor, defined in Eq. (8) for the helically coiled tube under test is reported vs. the Reynolds number.

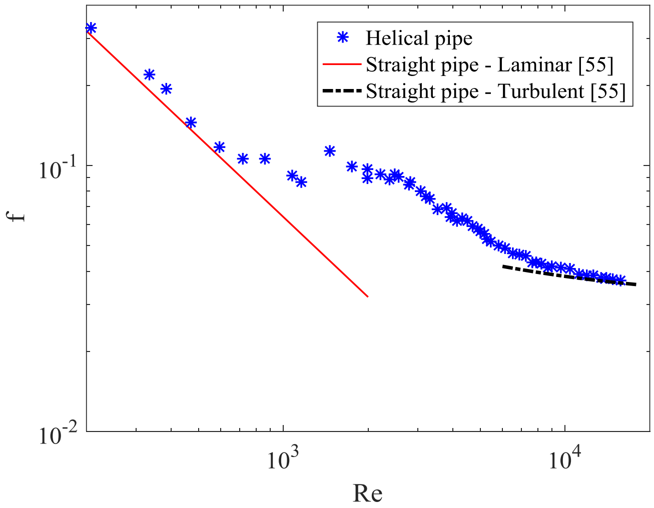

Figure 5. Darcy friction factor vs. Reynolds number for the helically coiled tube under test and comparison with the behaviour in a straight pipe.

In the same figure the analytical solution for the laminar fully developed flow, holding for the straight tube is reported [55] together with the distribution of the Darcy friction factor for turbulent regime in a straight pipe.
The pressure drop study gives several information about the transition from laminar to turbulent regime in coiled pipes. First of all, the data confirm that, as observed by several authors [10,11], the transition to turbulence is more gradual than in straight pipes and exhibits a more complex behavior. The friction factor presented various discontinuity in its slope and the transitions seems to be characterised by different intermediate steps [10,11]. A first change in the friction factor trend appears in correspondence of $Re \approx 600$ probably due to the fact that the intensity of the secondary flow induced by the centrifugal force starts to become significant; then it is possible to notice another change of slope in correspondence of approximately $Re \approx 2500$ and a third one in the range $6000 < Re < 7000$. These last two discontinuities could be interpreted as the beginning and ending of the transition. This evidence is in partial agreement with the correlations proposed by Cioncolini and Santini [11] and by Ito [15] that suggest, for the geometry considered in this work, a critical Reynolds number value in the range $6000 < Re_{cr} < 7500$. Anyway, pressure drop distribution analysis doesn't enable to identify exactly the beginning and ending of the transition.

3.2 Local convective heat transfer coefficient

A further insight into the phenomena correlated to the transition from the laminar to the turbulent flow regime in coiled pipes was found in the analysis of the distribution of the convective heat transfer coefficient along the wall circumference.
This information was hereby derived by solving the linear IHCP in the tube wall by adopting the temperature infrared maps on the external coil wall as input data.

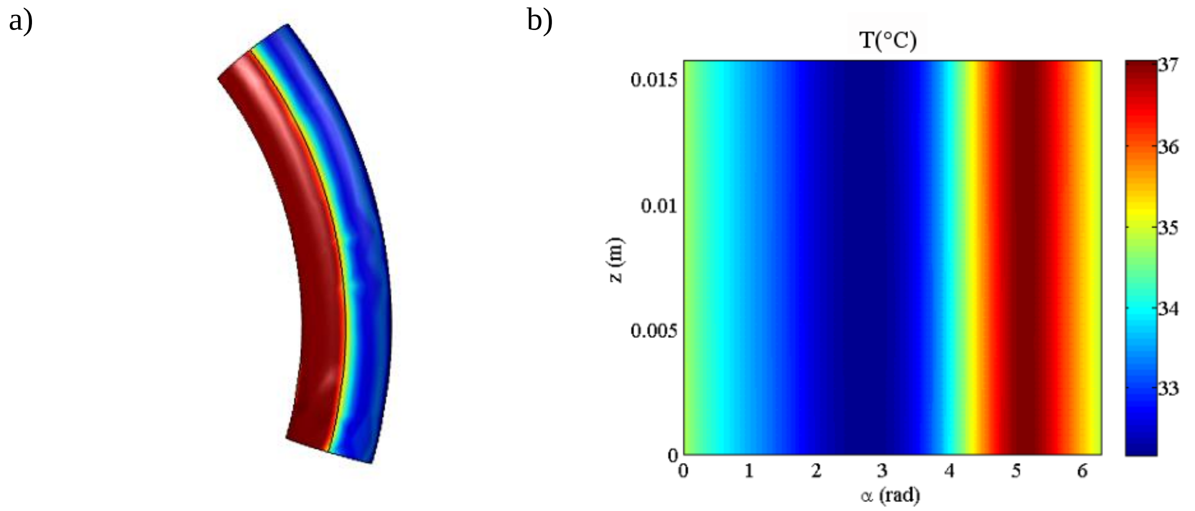

Figure 6. A 3D view of the temperature distribution at the test section (a) and the corresponding temperature unwrapped distribution on the tube wall versus the circumferential angular coordinate (b) for the *Re*=364 case.

Fig. 6a reports, for a representative case, the three-dimensional representation of the temperature distribution at the test section. In Fig. 6b the corresponding temperature unwrapped distribution on the tube wall versus the circumferential angular coordinate is reported.

These data clearly reveal that the temperature distribution exhibits significant variations along the circumference, while the temperature gradient is almost negligible along the axis of the pipe. This observation confirms that adopting a 2-D numerical model for this type of problem is appropriate for the condition under test.
The relative temperature distribution, defined as the difference between the wall and the bulk temperature, over the whole wall circumference is reported in Fig. 7 for three representative Reynold number values: the angular coordinate origin was taken at the inner side of the coil. For all the three Reynolds number values the temperature presents a distribution with a maximum in correspondence of the inner side of the coil where the axial velocity of the fluid, due to the centrifugal force is expected to be lower and thus also the heat transfer rate.

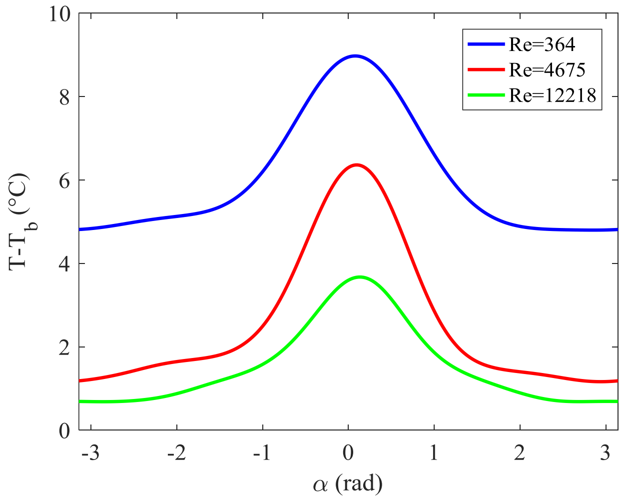

Figure 7. Relative temperature distributions on external wall of the coil.

The distributions of the Nusselt number restored by the estimation procedure presented above and divided by $Pr^{0.4}$ are reported in Fig.8 for the same three Reynolds number values of Fig.7

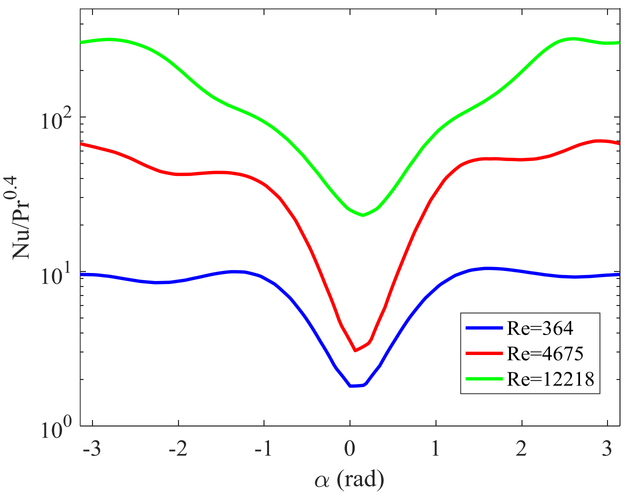

Figure 8. Restored Nusselt number distribution.

.

For all the three cases, the variation of the Nusselt number along the boundary of the duct section indicates that *Nu* reaches very low values close to the inner bend side of the coil, while it reaches significant high values at the outer bend side, due to the onset of the secondary flows induced by the wall curvature.
The data also show the effect of torsion induced by the coil pitch: the two vortices induced in the fluid flow by the wall curvature are not symmetrical [11].
To locally compare the heat transfer coefficient and Nusselt number distributions for the different *Re* values, the shifting effect of the torsion was compensated by introducing a relative angle α^* into the analysis, whose origin was taken where the heat transfer coefficient reaches its minimum. In Fig. 9 the $Nu/Pr^{0.4}$ distributions for Reynolds number values representative of laminar, transitional and turbulent flow regimes are reported.

Table 1: The 95% confidence interval of the main physical quantities involved in the estimation procedure

Y (K)	**α (°)**	***k* (W/m·K)**	$\boldsymbol{T_{env}}$ **(K)**	$\boldsymbol{R_{env}}$ **(m²·K/W)**	$\boldsymbol{q_g}$ **(W/m³)**	$\boldsymbol{T_b}$ **(K)**
±0.1 K	±4°	±5%	±0.1 K	±50%	±4%	±0.2 K

The accuracy associated with the estimated values was assigned by the parametric bootstrap method [56,57]: the input data of the estimation procedure are re-sampled from their respective probability distributions and, from these values, the unknowns are calculated by the estimation procedure presented above; this process is repeated many times, and the results are processed using standard statistical techniques for evaluating 95% confidence intervals. The assumed uncertainties in the input data are reported in Table 1.

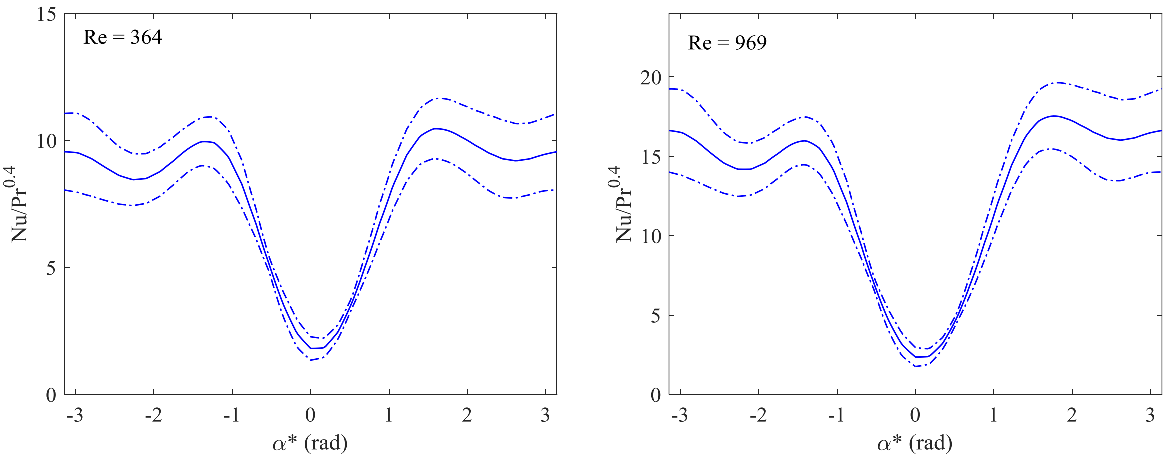

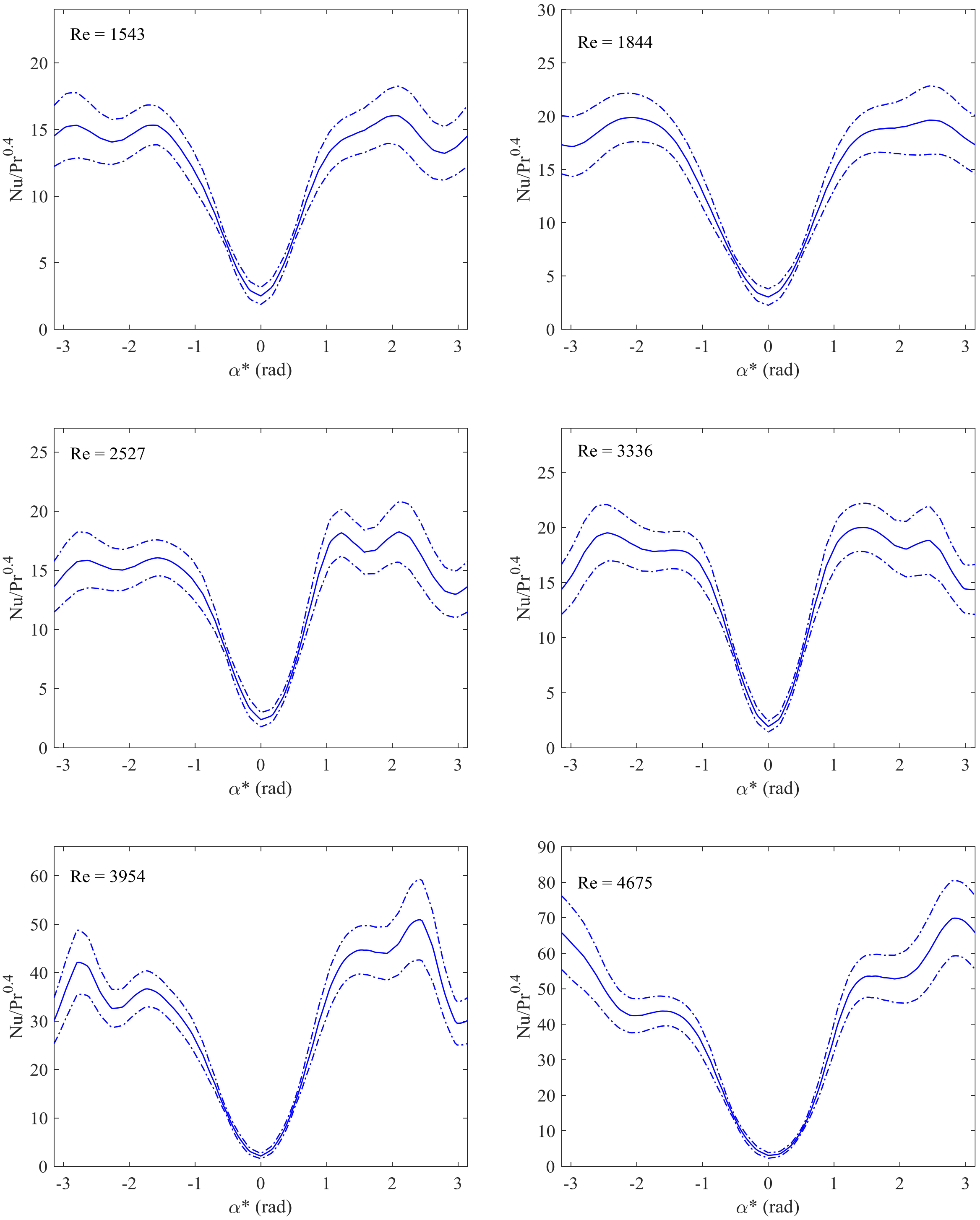
Re = 1543
Re = 1844
Re = 2527
Re = 3336
Re = 3954
Re = 4675
Nu/Pr^0.4
α* (rad)

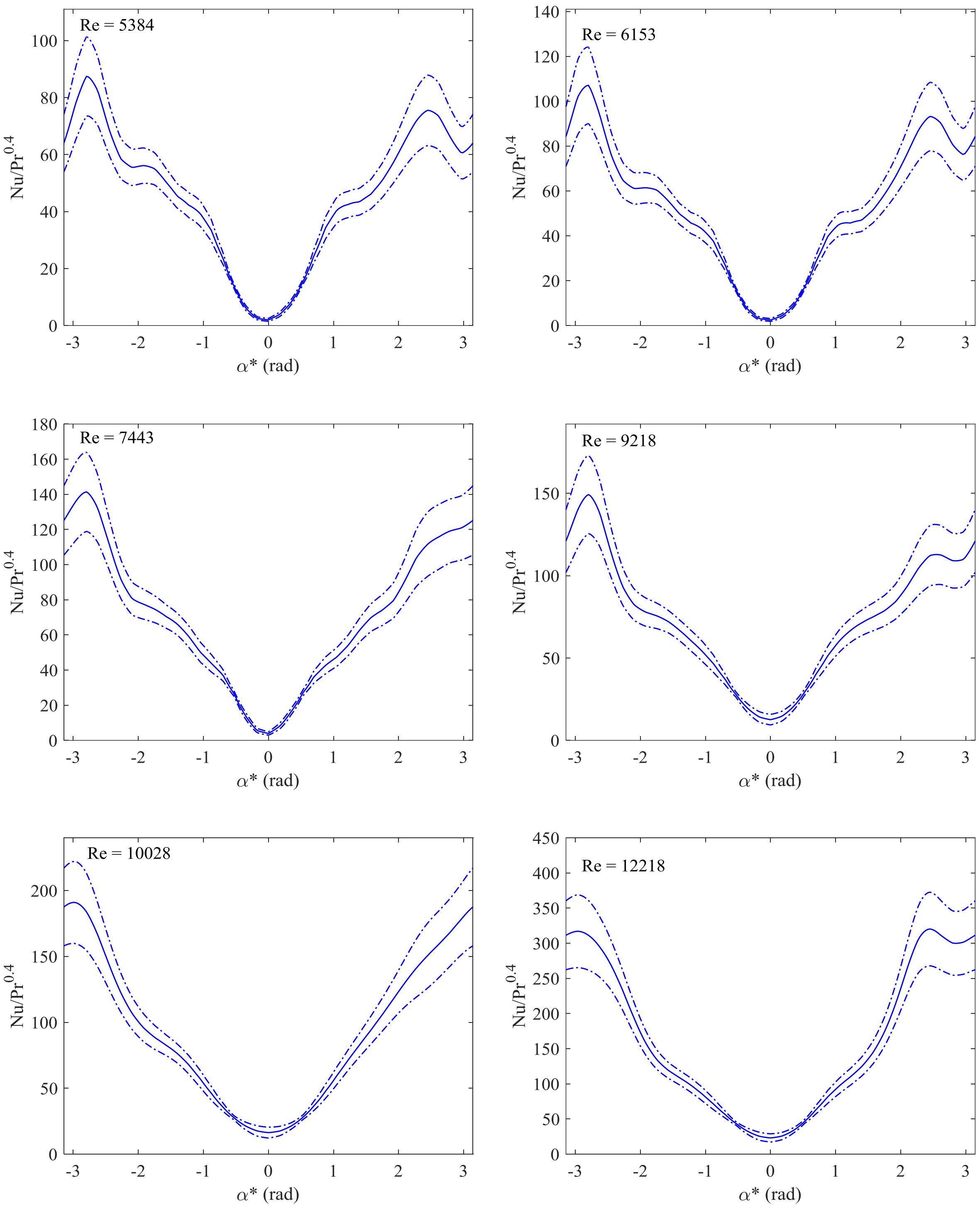

Figure 9. Restored $Nu/Pr^{0.4}$ distributions with a 95% confidence interval.

Before analysing the effects produced on the local convective heat transfer by the transitional flow regime, it is compulsory to study what happens both in laminar and in turbulent regimes. In order to compare the various distribution hereby obtained in the different test conditions, as suggested by Bozzoli et al. in [20], the Nu/Nu_{max} ratio is computed. In Fig. 10 it is analysed the laminar regime: the normalised Nusselt number distribution is reported for some representative cases for Reynolds number characteristics of the laminar regime and compared with the correlation obtained in the laminar regime in a previous study [20] where ethylene glycol was used as working fluid. By accounting for the experimental uncertainty, it can be stated that Nu/Nu_{max} ratio is almost independent from the Reynolds number and at the outside surface of the coil, the Nusselt number is approximately five times the one at the inside surface. It could be noticed that the pattern is particularly sharp and Nu/Nu_{max} is above 0.8 for approximately 75% of the circumference.

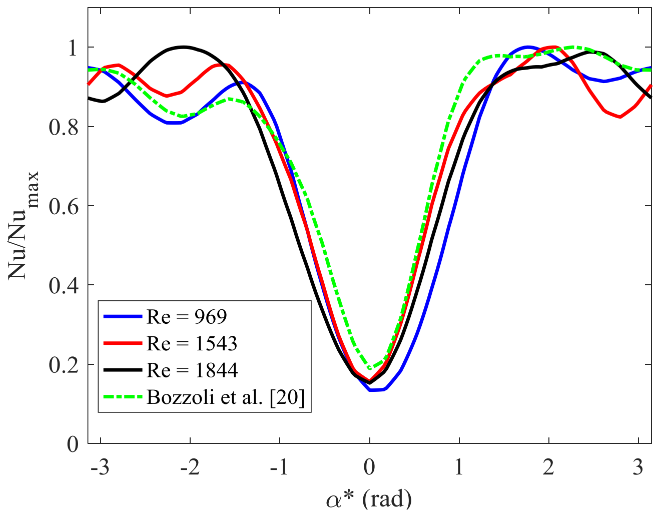

Figure 10. Normalised local Nusselt number for laminar flow regime.

Fig. 11 instead, reports the Nu/Nu_{max} ratio for various Reynolds number values characteristics of the turbulent flow regime: by accounting for the experimental uncertainty, it can be stated that, analogously to the laminar fluid flow case, this ratio is almost independent of the Reynolds number also for this flow condition, as observed by Jayakumar et al. [32].

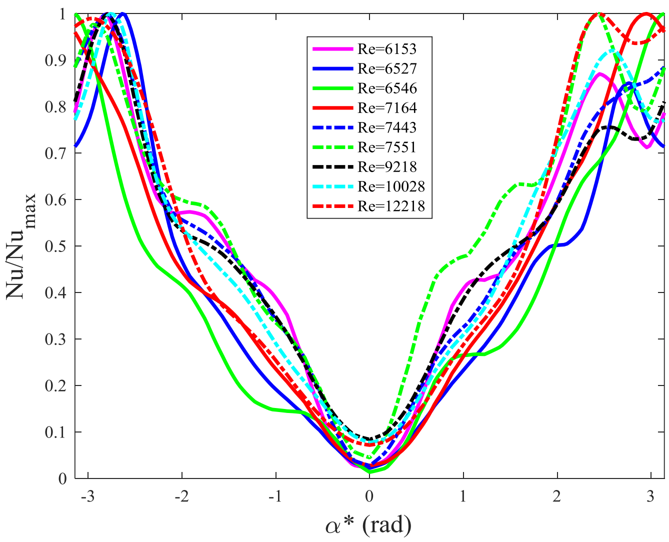

Figure 11. Normalised local Nusselt number for the turbulent flow regime.

The best fit of these experimental Nu/Nu_{max} distributions is plotted in Fig. 12 along with the distribution found for the laminar regime in [20]. Some differences between the two behaviours can be observed: in the turbulent regime, at the outside surface of the coil, the Nusselt number is about ten times larger than that at the inside surface while in the laminar regime it is only five time larger.

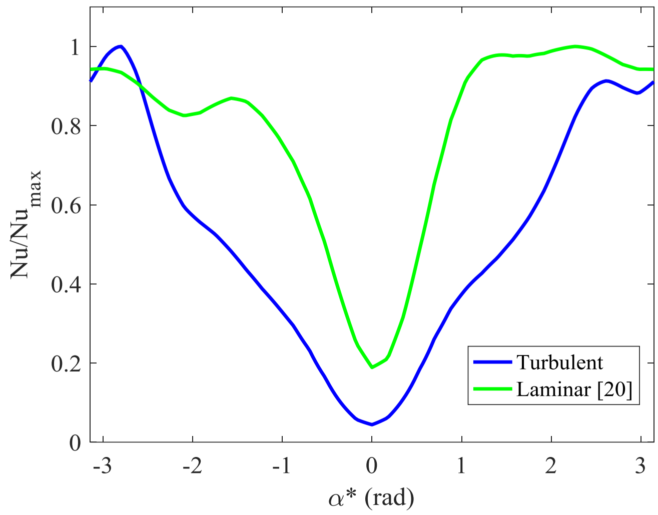

Figure 12. Comparison between the normalised local Nusselt number pattern in the laminar [20] and the turbulent flow regime.

Moreover, in turbulent regime the Nu/Nu_{max} pattern shows a typical "V-shape" profile while in the laminar regime the pattern is more flat near the outside surface of the coil.

This result is somewhat unexpected for the turbulent regime, where a more uniform heat transfer coefficient distribution is awaited, due to the fluid mixing produced by turbulence. This means that the fluid mixing promoted by turbulence is overcome by the distortion effect produced by the centrifugal force. This uneven distribution was somewhat observed by Di Liberto et al. [56]: by conducting a numerical study on turbulence in coiled pipes the Authors found out that turbulent fluctuations were clearly more intense near the outer region, where they were comparable in amplitude with those characteristic of the straight tube. On the inner wall they observed much lower fluctuations and they suggested that the flow remains laminar longer.

Then, considering Figs. 10-12, it is clear that laminar and turbulent regimes are characterised by different specific shapes of the local convective heat transfer coefficient distribution. In Fig. 13 the Nu/Nu_{max} ratio for four representative Reynolds numbers in the transitional flow regime (Reynolds number range 2500-6000) is reported together with the best fit of the data associated to the laminar [20] and turbulent regime.

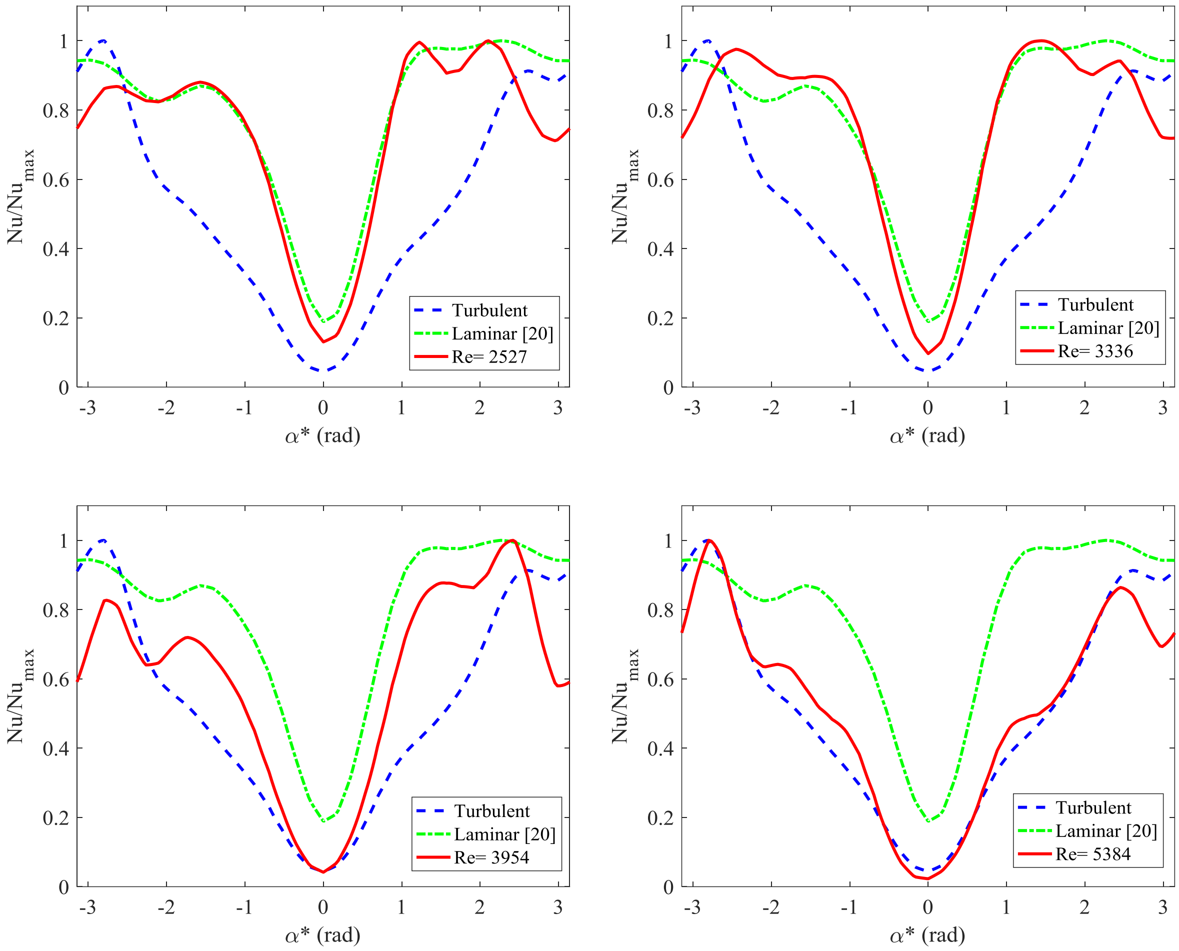

Figure 13. Normalised local Nusselt number and comparison with the data for the laminar [20] and turbulent regimes.

As it was highlighted by different Authors [10-16] and also as confirmed by the data reported in Section 4.1, the transition to turbulence doesn't seem to be as abrupt as in straight pipes but intermediate stages in the flow seems to occur. There isn't neither a sudden appearance nor a rapid development of turbulence and this is probably the reason why the only analysis of pressure drops doesn't allow to properly identify the starting of the turbulence: the turbulence emergence is so gradual that the only discontinuity that can be observed in friction factor profile marks the end of the process [11].

The results of Fig. 13 clearly show the gradual transition between the two behaviors: with the progression of the Reynolds number, the *Nu* profile approaches the "V-shape" pattern typical of the turbulent flow regime. At first an oscillating behavior is observed in correspondence of the outer bend accompanied by an increasing of the ratio between the Nusselt number at the outer position with respect to that at the inner position. This could be interpreted, as suggested by Di Piazza and Ciofalo [10], by the onset of an unsteadiness that interest the Dean vortex region. The ratio between the Nusselt number at the outer bend respect to that at the inner bend increases with the augmentation of the Reynolds number and the oscillating behaviour starts to affect a larger zone of the section. The increasing of the ratio could be interpreted, as suggested

[58], as a consequence of the fact that the turbulence emerges in correspondence of the outer bend while on the inner wall the flow remains laminar up to higher Reynolds number values.
Then finally the Nu/Nu_{max} distribution for $Re \approx 5400$ starts to present a pattern very close to the "V-shape" that characterized the turbulent flow regime.
The local Nusselt number distributions confirmes what was in part observed by the averaged friction factor (Fig. 5): in correspondence to approximately $Re \approx 6000$ for the hereby tested geometry the emergence of the turbulence occurs. Moreover, this powerful approach permits to add information regarding the different steps that occur in transitional flow regime in coiled pipes that are difficult to be highlighted by the classical methodologies of analysis based on the study of pressure drops.

5. Conclusion

In this paper, the local convective heat transfer coefficient distribution analysis is proposed as a complementary and detailed tool to investigate the transitional flow regime in coiled pipes.
In the majority of the papers available in the scientific literature, the transition to turbulence in curved pipes has been investigated on the basis of pressure drop behaviour but this approach showed some limits which have been overcome by the new methodology presented in this work.
In the present analysis, the temperature distribution maps on the external coil wall were employed as input data of the IHCP in the wall and a solution approach based on the Tikhonov regularisation method is implemented to restore the local convective heat transfer coefficient.
At first, local heat transfer behaviour in laminar and turbulent flow regimes was studied and some differences were found between the two regimes: in the turbulent regime, at the outside bend of the coil, the Nusselt number is about ten times larger than that at the inner bend while in the laminar regime it is only five time larger; in turbulent regime the Nu/Nu_{max} pattern shows a typical "V-shape" while in the laminar regime the pattern is more flat near the outer bend side of the coil.
Then the transitional regime was analysed and the results clearly showed the gradual transition between the two behaviors: transition to turbulence is not as abrupt as in straight pipes but intermediate stages in the flow occur and with the progression of the Reynolds number, the Nu/Nu_{max} profile gradually approaches the "V-shape" pattern of the turbulent flow regime where the rate of production of fluctuations is expected to exceed the rate of damping due to the centrifugal force.
The present analysis demonstrates that the IHCP approach provides very interesting and promising tools for detecting and studying complex phenomena such as the transition between the laminar and turbulent flow regimes. Moreover, it permits to add information regarding the different steps that occur in transitional flow regime in coiled pipes that are difficult to be highlighted by the classical methodologies based on average heat transfer or pressure drop measurements.
Eventually, these data could be employed also as a useful benchmark for CFD results and in the design of coiled tube heat exchangers as well.

Acknowledgments

This work was partially supported by the Emilia-Romagna Region (POR-FESR 2014-2020). MBS S.r.l. (Parma, Italy) is gratefully acknowledged for the set-up of the experimental apparatus.

Nomenclature

Symbol	**Quantity**	**SI Unit**
c_p		J/kg·K
D	Tube diameter	m
f	Darcy friction factor	
h	Convective heat-transfer coefficient	$W/m^2 \cdot K$
k	Thermal conductivity	W/mK
l	Coil pitch	m
p	Pressure	Pa
$\dot{m}$	Mass flowrate	kg/s
q	Convective heat flux per unit area	W/m^2
q_g	Internal heat generation per unit area	W/m^2
r	Radial coordinate	m
w	Mean axial velocity	m/s
z	Axial coordinate	m
De	Dean number	
Nu	Nusselt number	
Re	Reynolds number $Re=\rho \cdot w \cdot D/\mu$	-
T	Temperature	K
Q	Convective Heat flux	W
R_{env}	Overall heat-transfer resistance between the external tube wall and the surrounding environment	$m^2 \cdot K$ / W
Nu	Nusselt number	
α	Angular coordinate	rad
δ	Curvature ratio	
μ	Dinamic viscosity	Pa·s
ρ	Density	Kg/m^3
Subscripts,superscripts		
b	Bulk	
e	Entrance	
env	Environment	
ext	External	
f	Fluid	
int	Internal	

References

[1] R. Webb, N.H. Kim, Principles of Enhanced Heat Transfer, 2nd ed., Taylor & Francis, New York, 2005.

[2] A.E. Bergles, Techniques to enhance heat transfer in: Handbook of Heat Transfer, McGraw-Hill, New-York, 1998.

[3] P. Naphon, S. Wongwises, A review of flow and heat transfer characteristics in curved tubes, Renewable and Sustainable Energy Reviews 10 (5) (2006) 463-490.

[4] S. Vashisth, V. Kumar, K. D. P. Nigam, A Review on the Potential Applications of Curved Geometries in Process Industry, Ind. Eng. Chem. Res. 47 (2008) 3291-3337.

[5] S. Rainieri, F. Bozzoli, L. Cattani, G. Pagliarini, Experimental investigation on the convective heat transfer enhancement for highly viscous fluids in helical coiled corrugated tubes, Journal of Physics: Conference Series 395 (2012), Paper No. 012032.

[6] W. R. Dean, Note on the motion of fluid in a curved pipe. Phil. Mag. 4 (1927) 208–223.

[7] W. R. Dean, The streamline motion of fluid in a curved pipe. Phil. Mag. 7 (1928) 673–695.

[8] F. Bozzoli, L. Cattani, S. Rainieri, G. Pagliarini, Estimation of local heat transfer coefficient in coiled tubes under inverse heat conduction problem approach, Experimental Thermal and Fluid Science 59 (2014) 246-251.

[9] L. Cattani, D. Maillet, F. Bozzoli, S. Rainieri, Estimation of the local convective heat transfer coefficient in pipe flow using a 2D thermal quadrupole model and truncated singular value decomposition, International Journal of Heat and Mass Tansfer 91 (2015) 1034-1045.

[10] I. Di Piazza, M. Ciofalo, Transition to turbulence in toroidal pipes, Journal of Fluid Mechanics 687 (2011) 72-117.

[11] A. Cioncolini, L. Santini, An experimental investigation regarding the laminar to turbulent flow transition in helically coiled pipes, Experimental Thermal and Fluid Science 30 (2006) 367-380.

[12] C.M. White, Streamline flow through curved pipes, Proceedings of the Royal Society of London, Series A 123 (1929) 645-663.

[13] J. Kühnen, M. Holzner, B. Hof, H.C. Kuhlmann, Experimental investigation of transitional flow in a toroidal pipe, Journal of Fluid Mechanics 738 (2014) 463-491.

[14] D.R. Webster, J.A.C. Humphrey, Experimental observations of flow instability in a helical coil, Journal of Fluids Engineering 115 (1993) 435-443.

[15] H. Ito, Friction factors for turbulent flow in curved pipes, Transactions of the Asme: Journal of Basic Engineering 81(1959) 123-134.

[16] S. Srinivasan, S. Nadapurkar, F.A. Holland, Friction factors for coils, Transactions of the Institution of Chemical Engineers 48 (1970) 156-161.

[17] S. Rainieri, F. Bozzoli, L. Cattani, G. Pagliarini, Compound convective heat transfer enhancement in helically coiled wall corrugated tubes, International Journal of Heat and Transfer 59 (2013) 353-362.

[18] R.C. Xin, M.A. Ebadian, The effects of Prandtl numbers on local and average convective heat transfer characteristcs in helical pipes, Journal of Heat Transfer 119 (3) (1997) 467-473.

[19] C. Yildiz, Y. Biçer, D. Pehlivan, Heat transfer and pressure drops in a heat exchanger with a helical pipe containing inside springs, Energy Convers Manage 38 (1997) 619-624.
[20] F. Bozzoli, L. Cattani, S. Rainieri, F.S.V. Bazan, L.S. Borges, Estimation of the local heat-transfer coefficient in the laminar flow regime in coiled tubes by the Tikhonov regularisation method, International Journal of Heat and Mass Transfer 72 (2014) 352-361
[21] B. Bai, L. Guo, Z. Feng, X. Chen, Turbulent Heat Transfer in a Horizontal Helically Coiled Tube, Heat Transfer-Asian Research 28(5) (1999) 395–403.
[22] R. A. Seban, E. F. McLaughlin, Heat transfer in tube coils with laminar and turbulent flow, International Journal of Heat and Mass Transfer 6 (1963) 387-395.
[23] L. A. M. Janssen, C. J. Hoogendoorn, Laminar convective heat transfer in helical coiled tubes, International Journal of Heat and Mass Transfer 21 (1978) 1197-1206.
[24] M. Akiyama, K. C. Cheng, Boundary vorticity method for laminar forced convection heat transfer in curved pipes, International Journal of Heat and Mass Transfer 14 (1971) 1659-1675.
[25] S. V. Patankar, V. S. Pratap, D. B. Spalding, Prediction of laminar flow and heat transfer in helically coiled pipes, Journal of Fluid Mechanics 62 (1974) 539-551.
[26] K. Futagami, A. Yoshiyuki, Laminar heat transfer in a helically coiled tube, International journal of heat and mass transfer 31 (1988) 387-396.
[27] L. Shijie, J.H. Masliyah, Developing convective heat transfer in helical pipes with finite pitch, International journal of heat and fluid flow 15 (1994) 66-74.
[28] G. Yang, M.A. Ebadian, Perturbation solution for laminar convective heat transfer in a helix pipe, Journal of heat transfer 116 (1994) 771-775.
[29] G. Yang, Z.F. Dong, M.A. Ebadian, Laminar forced convection in a helicoidal pipe with finite pitch, International Journal of Heat and Mass Transfer 38 (1995) 853-862.
[30] B. Zheng, C.X. Lin, M.A. Ebadian, Combined laminar forced convection and thermal radiation in a helical pipe, International journal of heat and mass transfer 43 (2000) 1067-1078.
[31] C.X. Lin, M.A. Ebadian, Developing turbulent convective heat transfer in helical pipes, International Journal of Heat and Mass Transfer 40 (1997) 3861-3873.
[32] J.S. Jayakumar, S.M. Mahajani, J.C. Mandal, N.I. Kannan, P.K., CFD analysis of single-phase flows inside helically coiled tubes, Computers & chemical engineering 34 (2010) 430-446.
[33] I. Di Piazza, M. Ciofalo, Numerical prediction of turbulent flow and heat transfer in helically coiled pipes, International Journal of Thermal Sciences 49 (2010) 653-663.
[34] Y.M. Ferng, W.C. Lin, C.C. Chieng, Numerically investigated effects of different Dean number and pitch size on flow and heat transfer characteristics in a helically coil-tube heat exchanger, Applied Thermal Engineering 36 (2012) 378-385.
[35] M. Di Liberto, M. Ciofalo, A study of turbulent heat transfer in curved pipes by numerical simulation, International Journal of Heat and Mass Transfer 59 (2013) 112-125.
[36] J.V. Beck, K. Arnold, Parameter Estimation in Engineering and Science, Wiley Interscience, New York, 1977.

[37] J.V. Beck, B. Balckwell, Jr C.R. St.Clair, Inverse Heat Conduction – Ill-posed problems, John Wiley & Sons Inc, New York, 1985.
[38] H.R.B. Orlande, F. Olivier, D. Maillet, R.M. Cotta, Thermal measurements and inverse techniques, Taylor and Francis, New York , 2011.
[39] O. M. Alifanov, Inverse Heat Transfer Problem, Springer, Berlin, 1994.
[40] O.M. Alifanov, Solution of an inverse problem of heat conduction by iteration methods, Journal of Engineering Physics , 26 (4) (1974) 471–476.
[41] D.A. Murio, The Mollification Method and the Numerical Solution of Ill-Posed Problems, John Wiley and Sons, New York, 1993.
[42] F. Bozzoli, G. Pagliarini, S. Rainieri, Experimental validation of the filtering technique approach applied to the restoration of the heat source field, Experimental Thermal and Fluid Science 44 (2013) 858-867.
[43] H. Massard, H.R.B. Orlande, O. Fudym, Estimation of position-dependent transient heat source with the Kalman filter, Inverse Problems in Science and Engineering 20 (7) (2012) 1079-1099.
[44] F. Bozzoli, L. Cattani, G. Pagliarini, S. Rainieri, Infrared image filtering applied to the restoration of the convective heat transfer coefficient distribution in coiled tubes, Opto-electronics Review 23 (1) (2015) 109-117.
[45] S. K. Kim, W. I. Lee, Solution of inverse heat conduction problems using maximum entropy method, International Journal of Heat and Mass Transfer 45 (2002) 381-391.
[46] A.N. Tichonov, V.Y. Arsenin, Solution of Ill-posed Problems, Winston & Sons, Washington, 1977.
[47] Bozzoli, F., Cattani, L., Corradi, C., Mordacci, M. and Rainieri, S., Inverse estimation of the local heat transfer coefficient in curved tubes: a numerical validation, Journal of Physics: Conference Series (Vol. 501, No. 1, p. 012002). IOP Publishing, 2014.
[48] P.C. Hansen, Truncated singular value decomposition solutions to discrete illposed problems with ill-determined numerical rank, SIAM Journal on Scientific and Statistical Computing 11 (1990) 503–518.
[49] P.C. Hansen, Rank-deficient and discrete ill-posed problems, SIAM, Philadelphia, 1998.
[50] M. D'Oria, P. Mignosa, M.G. Tanda, Evaluation of the flow released from a levee breach through a Bayesian inverse methodology, River Flow 2016 CRC Press (2016) 1958-1966.
[51] H.R.B. Orlande, M.J. Colaço and G. S. Dulikravich, Approximation of the likelihood function in the Bayesian technique for the solution of inverse problems, Inverse Problems in Science and Engineering 16.6 (2008) 677-692.
[52] F.S.V. Bazán, Fixed-point iteration in determining the Tikhonov regularization parameter, Inverse Problems 24 (2008), 035001.
[53] F.S.V. Bazan, L.S. Borges, GKB-FP: an algorithm for large-scale discrete ill-posed problems, Bit Numerical Mathematics 50(3) (2010) 481-507.
[54] R.K. Shah, A.L. London, Laminar Flow Forced Convection in Ducts, Academic Press, 1978.
[55] F.P. Incroprera, D.P. De Witt, Fundamentals of Heat and Mass Transfer, John Wiley& Sons, Inc New York, 2002.

[56] B. Efron, The jackknife, the bootstrap and other resampling plans, Society of Industrial and Applied Mathematics CBMS-NSF Monographs, Philadelphia, 1982.
[57] B. Blackwell, J.V. Beck, A technique for uncertainty analysis for inverse heat conduction problems, International Journal of Heat and Mass Transfer 53(4) (2010).
[58] Di Liberto M., Di Piazza I., Ciofalo M., Turbulence structure and budgets in curved pipes, Computer & Fluids 88 (2013) 452-472.